Attenuation properties of electrically large periodic structures applying FEM

Werner Renhart[1], Christian Tuerk[2], Thomas Bauernfeind[1], and Christian A. Magele[1]

[1]Institute for Fundamentals and Theory in Electrical Engineering, Graz University of Technology, 8010 Graz, Austria
[2]Armament and Defence Technology Agency, Ministry of Defence and Sports, 1090 Vienna, Austria

Avoiding electromagnetic field contamination of large rooms is a very cumbersome and expensive task, especially when a widespread frequency range has to be considered. Often, windows serve as vents. This implies the use of absorbing structures with electrically large feedthroughs at a certain mechanical robustness. In this paper the attention has been drawn to metallic, periodic structures like arrays of rectangular waveguides. Electromagnetic waves at different incident angles strike the structure whereas the influence of its thickness will be varied, as well. The prescription of the attenuation properties will be given. All results will be achieved with the aid of finite element computations.

***Index Terms*—HF-shielding, absorbing structures, electromagnetic compatibility, finite elements**

I. Introduction

In many real life situations large rooms of more or less perfect cleanness of electromagnetic fields are required, eg. electron microscopy laboratories. At the same time an entire accessibility to wireless communication networks must be ensured. Modern routers and access point equipments are broadcasting the communication networks in dual bands, that is actually 5.0 and 2.4 GHz. Near future technologies will use even higher frequencies therefore. Careful designed screening measures should be considered, already in the planning phase of critical buildings and rooms.

So, perfect metallic enclosures often can not be put into practize due to practical constraints like the integration of vents, incidence of daylight or voluminous wall ducts. At such surfaces the use of metallic wave guides assembled to a periodic structure may achieve both, a required shielding effect, acceptable light admission as well as a sufficient air flow through vents. An idea of such a basic structure is illustrated in Fig. 1. Quadratic wave guide tubes of a distinct length are stacked and serve for the requested structure.

Obviously, the fill-up of a window with such a structure ends in a length (indicated in Fig. 1) of tens of centimetres. Hence the structure becomes electrically long in terms of free space wave lengths for the GHz-frequency range. This and the high conductivity of the material (metallic walls) is a real drawback while evaluating its attenuation behaviour numerically. Any simulation operating with material homogenization, as pointed out, eg. in [1], [2] will fail. Neither the treatment as a frequency selective surface [3] will succed. This necessitates the computation of fully 3-D periodic structured models.

II. FEM-formulation and modeling

We have to face a wave propagation problem at the coexistance of highly conducting materials. Thereby, the problem of modeling a non-perpendicularly impinging plane wave arises

Manuscript received June, 2013; Corresponding author: W. Renhart (email: werner.renhar@tugraz.at).

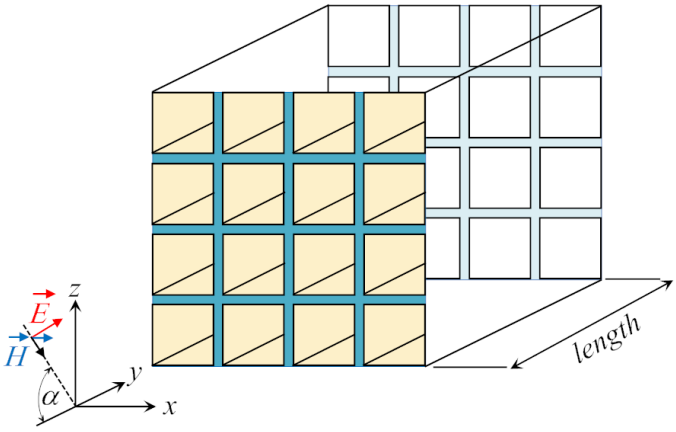

Fig. 1. Basic arrangement, impinging plane wave indicated at an incident angle α, variable thickness.

which is outlined in the basic arrangement in Fig. 1. As consecutively outlined a suitable way to model the impinging plane wave is the choice of the magnetic vector potential $\vec{A}$ together with the electric scalar potential v. Additionally, a FE-mesh truncation behind the shielding structure with the aid of impedance boundary conditions in terms of the mentioned potentials becomes conveniently.

A. FEM-formulation

In the well known $\vec{A}v$-formulation (eg. [4]) the electric field intensity $\vec{E}$ and the magnetic field density $\vec{B}$ with the potentials in use become

$$\vec{E} = -j\omega\vec{A} - j\omega\nabla v, \quad \vec{B} = curl\vec{A}. \tag{1}$$

Assuming time harmonic variations of the field quantities, the current density $\vec{J}$ can be expressed by [6]

$$\vec{J} = (\sigma + j\omega\epsilon)\vec{E}. \tag{2}$$

With the electric conductivity σ the conductor currents in the matallic walls are comprised whereas the displacement current

density is considered by the remaining $\jmath\omega\epsilon$-part. ϵ being the dielectric permittivity. Applying to the governing equations

$$\nabla \times (\frac{1}{\mu}\nabla \times \vec{A}) + (\sigma + j\omega\epsilon)j\omega(\vec{A} + \nabla v) = \vec{0} \quad (3)$$

$$\nabla \cdot (\sigma + j\omega\epsilon)j\omega(\vec{A} + \nabla v) = 0 \quad (4)$$

the Galerkin wighted residual method, the weak form of (3) becomes:

$$- \int_\Omega \nabla \times \vec{N}_i \cdot \frac{1}{\mu}\nabla \times \vec{A} d\Omega + \int_{\Gamma_{tr}} \vec{N}_i \cdot \underbrace{(\vec{n} \times (\frac{1}{\mu}\nabla \times \vec{A}))}_{\vec{n}\times\vec{H}} d\Gamma$$

$$+ \int_\Omega \vec{N}_i \cdot (\sigma + j\omega\epsilon)j\omega(\vec{A} + \nabla v) d\Omega = 0. \quad (5)$$

Therein, μ stands for the magnetic permeability and $\vec{N}_i$ represents the set of the edge weighting functions. The Neumann integral term in (5) serves for the implementation of the impedance boundary conditions to truncate the mesh along Γ_{tr}. As can be seen in the underbraced term, the tangential of $\vec{H}$ can directly be substituted by the tangential of $\vec{E}$ to implement the wave impedance condition for free space

$$\vec{n} \times \vec{H} = \sqrt{\frac{\epsilon_0}{\mu_0}}\vec{E}_t \quad (6)$$

B. Incident wave modeling

To model the incident plane wave some basics should be brought up. The field situation at the front of the shielding structure with the co-ordinate system used is skatched in Fig. 2. A linearly polarised plane wave impinges the structure at

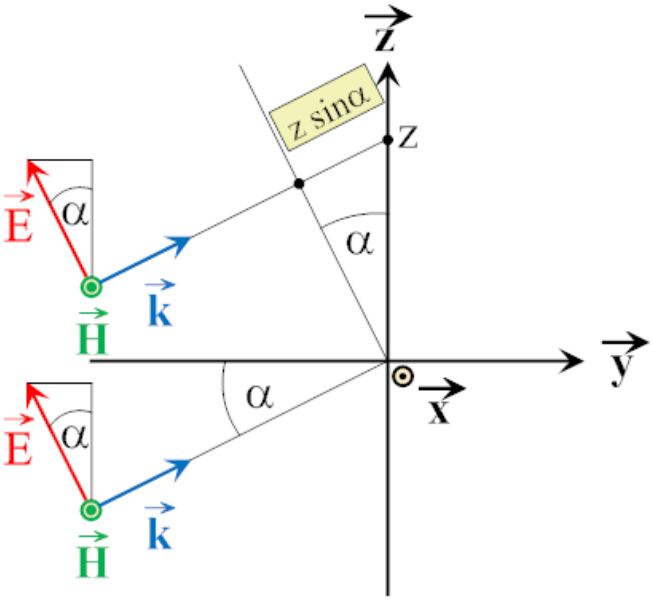

Fig. 2. Basic arrangement, impinging plane wave indicated at an incident angle α, variable thickness.

an angle α and the electric field $\vec{E}$ is orientated vertically (yz-plane). Its z-component can be written as

$$E_z(\vec{r}, t) = \hat{E} \cos\,\alpha\, e^{j(\omega t - \vec{r}\cdot\vec{k})}. \quad (7)$$

$\hat{E}$ represents the maximum value of $\vec{E}$ and $\vec{r}$ corresponds to the space co-ordinates. The wave vektor $\vec{k}$ and the plane spanned by $\vec{E} \times \vec{H}$ are orthogonal. $\vec{k}$ correlates to the positive wave propagation direction. According to the indicated co-ordinate system the vectors $\vec{k}$ and $\vec{r}$ have the form

$$\vec{k} = \frac{\omega}{c}\begin{pmatrix} 0 \\ \cos\alpha \\ \sin\alpha \end{pmatrix}, \qquad \vec{r} = \begin{pmatrix} 0 \\ 0 \\ z \end{pmatrix}. \quad (8)$$

c denotes the medium velocity which in our case corresponds to the light velocity in vacuum. With this and accomplishing the dot-product, (7) becomes

$$E_z(\vec{r}, t) = \hat{E} \cos\,\alpha\, e^{j(\omega t - \frac{\omega}{c} z \sin\alpha)}. \quad (9)$$

Along the entrance plane of the structure the exponent in (9) depends on the co-ordinate value of z only and accounts for the phase difference along the plane. This condition now has to be incorporated into the FEM-formulation. At first, surfaces with plane wave prescriptions should be considered as equipotential surfaces with respect to the electric scalar potential v. Therewith the electric scalar v in (1) can be set to zero, hence the gradient term vanishes. Equation (1) simplifies to

$$\vec{E} = -j\omega\vec{A} \quad \mapsto \quad \vec{A} = -\frac{\vec{E}}{j\omega}. \quad (10)$$

Now, bearing the representation of $\vec{A}$ with edge basis functions in terms of $\vec{N}_k$ [5] in mind, it follows:

$$\vec{A} = \sum_{k=1}^{e} a_k \vec{N}_k. \quad (11)$$

Herein, e is the number of edges, $\vec{N}_k$ represents the k-th edge basis function. Applying (9) and (10) the values a_k can be obtained by evaluating the line integrals of $\vec{E}$ of the impinging electromagnetic wave along the $k-th$ edge in z-direction

$$a_k = -\frac{1}{j\omega}\int_k \hat{E} \cos\,\alpha\, e^{j(\omega t - \frac{\omega}{c} z \sin\alpha)}\, dl. \quad (12)$$

Finally, the values obtained for a_k can be treated as inhomogenous Dirichlet boundary conditions.

III. Numerical Investigations

A. Postcrocessing of the numerical results

The question arises at which points or along which plane the attenuation effect of the shielding structure should be benchmarked. Selecting a plane at the back end of the structure seemed to be meaningful, at first. Hence, we examined the field behaviour along a vertical plane at the end of the wave guide structure. We examined a configuration consisting of an array of 5×5 wave guides and a plane wave impinging to it with an incident angle of $45\ deg$ at $6\,GHz$. Fig. 3 shows the distribution of the maximum of $\vec{E}$ along the plane mentioned. Along this plane no superposition of the fields of the individual tubes can be observed.

So, in a next step we moved the plane $d = 5\,mm$ off. In Fig. 4 still the conturs of the wave guide tubes are visible. To avoid singularity effects in the field pattern due to the metallic wave

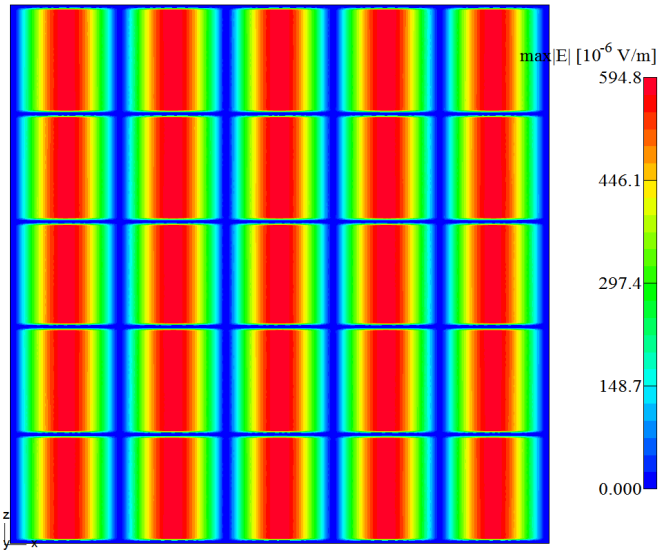

Fig. 3. Maximum of $\vec{E}$ along the plane at the end of the structure, 5x5 wave guides stacked.

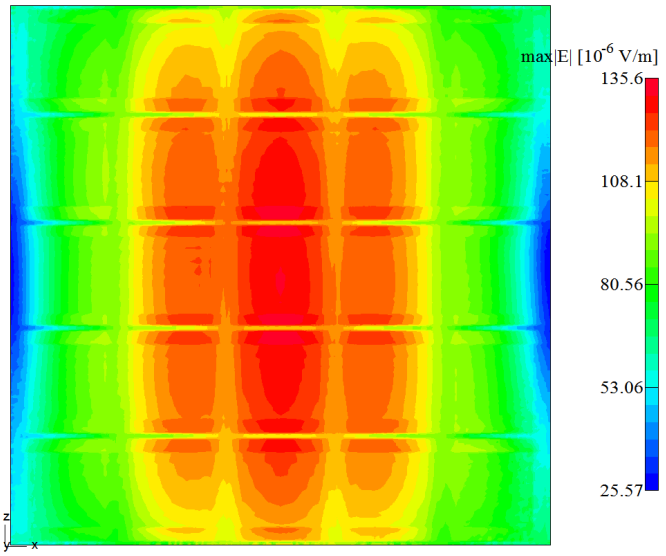

Fig. 4. Maximum of $\vec{E}$, plane $5\,mm$ behind the end of the structure.

guide edges we moved the plane to a distance of $d = 10\,mm$ away form the structure. The distribution of $|\vec{E}|_{max}$ at this plane (Fig. 5) appears smoothly. Now we found a final distance of $d = 10\,mm$ away form the structure. For all comparisons this plane of postprocessing has been kept unchanged.

B. Final structure and model parameters

For the huge amount of computations to be done, it had turned out, that an array of 5×5 wave guides will overkill our aims. Hence, an arrangement of 3x3 quadratic wave guide tubes has been selected to serve as the basic arrangement for our investigations (Fig. 6). The orange colored shielding structure is made of steel with a conductivity of $\sigma = 5 \cdot 10^6\, S/m$ and a relative permeability of $\mu_r = 100$. The inner tube size is $10 \times 10\,mm$ whereas the wall thickness amounts to $1\,mm$. At the back end of the structure an air region has

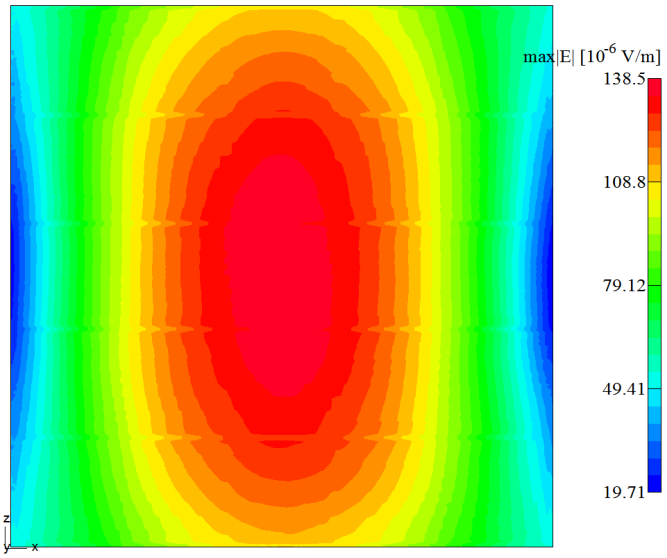

Fig. 5. Maximum of $\vec{E}$, final plane $10\,mm$ off the end of the structure.

been modeled, too. For all frequencies considered, the free space at least sizes to the double wavelength λ. On its outer bounds the impedance boundary conditions, as given in (6) have been prescribed to truncate the finite element mesh. Along a vertical plane (yellow in Fig. 6) situated at a constant distance of $d = 10\,mm$ behind the shielding structure the field quantities will be compared. As previously mentioned, due to communication requirements, the frequency range has been selected between $3\,GHz$ and $12\,GHz$.

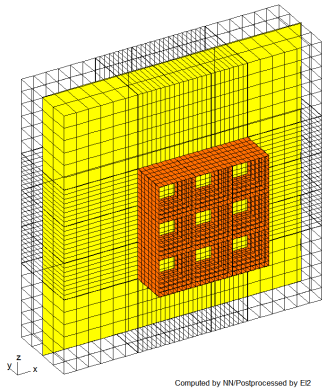

Fig. 6. FE-mesh of the basic arrangement, 3x3 quadratic wave guide tubes, plane of post-processing $10\,mm$ behind the structure.

C. Numerical results and comparison

The attenuation of the shielding structure given by

$$a_t|_{dB} = 20\,\log\frac{|\hat{E}_{out}|}{|\hat{E}_{in}|} \tag{13}$$

has been evaluated. $|\hat{E}_{in}|$, the maximum of the prescribed incident wave (12) always was $1\,V/m$ whereas $|\hat{E}_{out}|$ represents the maximum value of $\vec{E}$ appearing in the plane of postprocessing. At first, the frequency dependency of the

attenuation has been investigated. Fig.7 shows the shielding bahavior for a length of $l = 20\,mm$ of the tubes. In the next

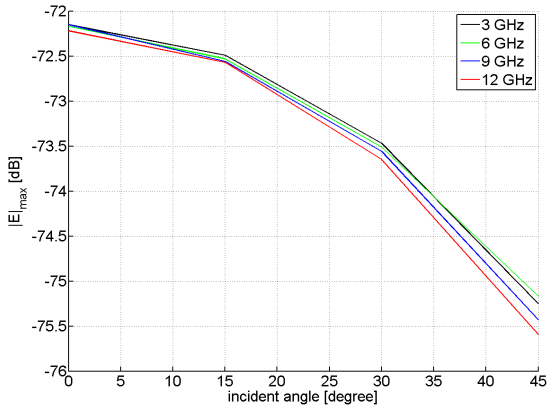

Fig. 7. Basic arrangement,length of tubes $l = 20\,mm$, attenuation at variant incident angle.

step, the tubes have been stretched to a length of $l = 80\,mm$ (Fig. 8). For both the short and the long structure a quite similar behavior can be seen. The absolute values only change. The same bahavior could be stated for any length l lying between the values shown. After this, the influence of the

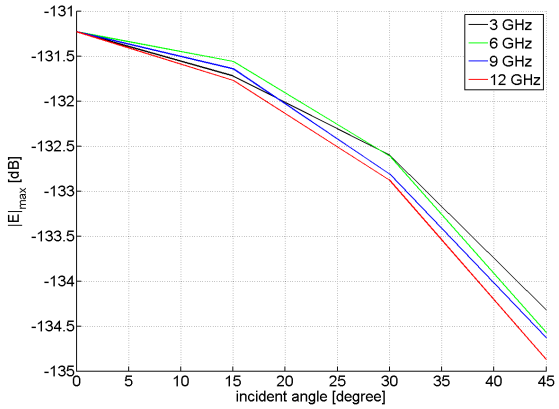

Fig. 8. Basic arrangement,length of tubes $l = 80\,mm$, attenuation at variant incident angle..

length l of the structure on the attenuation has been computed. Fig. 9 shows the results for the frequency $f = 3GHz$ at the incident angles $0\,deg$ and $45\,deg$. Finally the same investigations for the frequency of $f = 6GHz$ lead to the lines shown in Fig. 10.

IV. Conclusion

The paper describes a procedure for computing the attenuation behavior of periodical structures made of high conductive material. Due to mechanical reasons the length of such structures will become electrically long in terms of wavelengths. Hence, no homogenization procedure can be applied to model the structure conventiently. A method has been proposed how to excite a problem with skewed impinging plane waves while

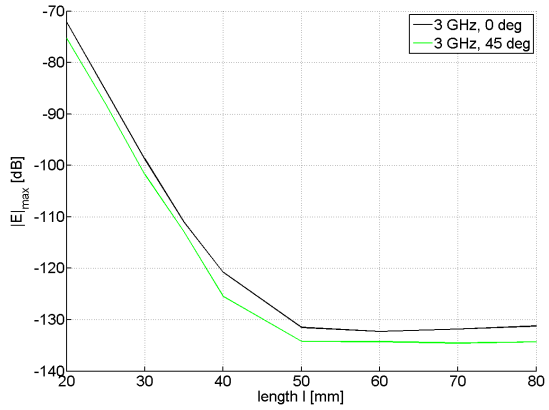

Fig. 9. Basic arrangement, 3x3 quadratic wave guide tubes, plane of post-processing 10 mm behind the structure.

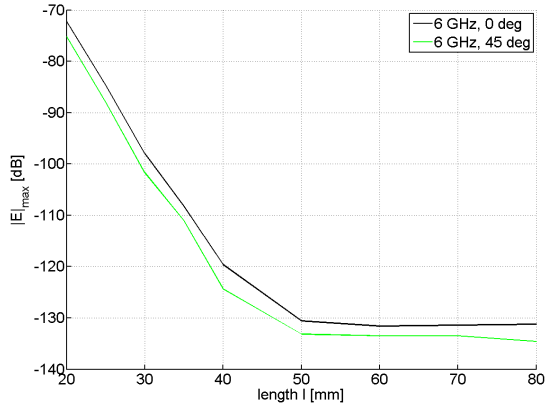

Fig. 10. Basic arrangement, 3x3 quadratic wave guide tubes, plane of post-processing 10 mm behind the structure.

using a vector potential edge presentation in the finite element formulation. For different length of the screening scructure and for variant incident angles the attenuation behavior has been discussed.

References

[1] Z. Peng, J. Wang, F. Lei, J. Lee, "New computational strategies for electromagnetic modeling of multiscale heterogeneous composites", 5th European Conference on Antennas and Propagation (EUCAP), *Proceedings*, 2011, pp. 3226-3229.

[2] M. Johansson, C.L. Holloway, E.F. Kuester, "Effective Electromagnetic Properties of Honeycomb Composites, and Hollow-Pyramidal and Alternating-Wedge Absorbers", *IEEE Trans. on Antennas and Prop.*, Vol. 53, No. 2, February 2005, pp. 728-736.

[3] I. Bardi, R. Remski, D. Perry, Z. Cendes, "Plane Wave Scattering From Frequency-Selective Surfaces by the Finite-Element Method", *IEEE Trans. Magn.*, Vol. 38, No. 2, March 2002, pp. 641-644.

[4] O. Bíró, "Edge element formulations of eddy current problems", *Computer methods in applied mechanics and engineering*, Vol. 169, 1999, pp. 391-405.

[5] O. Bíró, K. Preis, "Generating Source Field Functions With Limited Support for Edge Finite-Element Eddy Current Analysis", *IEEE Trans. on Magn.*, Vol. 43, No. 4, April 2007, pp. 1165-1168.

[6] W. Renhart, K. Hollaus, C. Magele, G. Matzenauer, B. Weiss, "Radiation of USB-WLAN antenna influenced by human tissue and by notebook enclosure", *IEEE Trans. on Magn.*, Vol. 43, No. 4, April 2007, pp. 1345-1348.